

Processing and characterisation of Pr–zircon pigment powder

J. K. Kar^{*1}, R. Stevens² and C. R. Bowen²

Praseodymium–zircon pigment powders were successfully prepared at different calcination temperatures with sodium fluoride NaF as mineraliser, using the solid state synthesis method. The powders were characterised using techniques such as XRD, SEM and TEM. Qualitative investigation of the phases using XRD showed the presence of large amounts of unreacted zirconia after calcination at 900 and 950°C, whereas from 1000 to 1200°C zircon was found to be the major phase, together with a small amount of zirconia. Quantitative investigation of phases was carried out using an external standard method. The weight fraction of unreacted zirconia at 1000°C was found to be 0·056. SEM observation of powders exposed at various calcination temperatures indicated the presence of tetrahedral crystals, and this was enhanced by the addition of the NaF mineraliser. TEM observations showed lattice defects and elastic strains in the samples at various calcination temperatures.

Keywords: Pigment, Praseodymium, X-ray diffraction, Zircon

Introduction

Natural and synthetic inorganic pigments produced and marketed as fine powders are an integral part of many decorative and protective coatings and are used for mass coloration of many materials including glazes, ceramic bodies and porcelain enamels.^{1–3} In such applications, the pigments are dispersed in the ceramic media, forming a heterogeneous mixture. Ceramic pigments or stains based on zircon are commonly used in industrial applications for glazes, owing to their high chemical durability, which gives the species superior resistance to dissolution during firing.^{4,5} One example of a synthetic inorganic pigment is zirconium praseodymium yellow, which belongs to the zircon pigment system.^{6–8} The present paper reports the first quantitative investigation of the amount of unreacted zirconia in the Pr–zircon system in conjunction with microstructural characterisation of the pigment powders at different calcination temperatures. Quantification of the weight fraction is important because the amount of unreacted zirconia can influence the colour intensity of the pigment powder as well as the final application within the glaze.

Experimental procedure

Sample preparation

Raw powders (ZrO_2 , SiO_2 , Pr_6O_{11}) for the manufacture of Pr–zircon yellow were mixed according to the

required chemical composition prior to ball milling for 1 h, using a high density polyethylene plastic bottle containing zirconia grinding media and distilled water as the liquid suspension. The main purpose of ball milling was to intimately mix the components to produce a homogeneous powder.

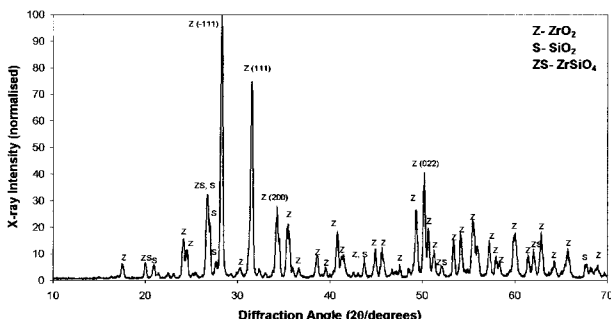
The milled powders were dried using an infrared lamp. A further milling stage was performed using a pestle and mortar to break up any soft agglomerates. Powders were then passed through a 150 µm size sieve. The sieved powders were placed in new, pure alumina/zirconia crucibles and subjected to calcination at different temperatures and for predetermined soaking times for reaction of the raw materials to take place and to allow incorporation of Pr_6O_{11} into the zircon host lattice. A dedicated carbolite muffle furnace was used for this purpose. A ramp rate of 300 K h⁻¹ was used during the heating cycle, and samples were furnace cooled after holding at the required temperature.

The prepared samples of Pr–zircon had the chemical composition $\text{Zr}_{0.95}\text{Pr}_{0.05}\text{SiO}_4$, with sample codes given in Table 1. Precursors used were ZrO_2 , SiO_2 and Pr_6O_{11} . NaF (5 wt-% of total mixture) was used as the mineraliser to aid the formation of the zircon lattice from the ZrO_2 and SiO_2 , effectively lowering the calcination temperatures. The raw materials ZrO_2 , SiO_2 , Pr_6O_{11} and NaF (99% pure) were supplied by Treibacher Auermet, Austria. During reaction, the colouring oxide species diffused into the lattice. Entrance of Pr^{3+} into the lattice occurs simultaneously with the $\text{ZrO}_2 + \text{SiO}_2$ reaction. This pigment is considered as a solid solution of Pr^{3+} cation in a zircon structure where Pr^{3+} replaces Zr^{4+} cations. Samples of Pr–zircon were heat treated at 900, 950, 1000, 1100 and 1200°C with 2 h soaking time. Samples gave an intense yellow colour after heat treatment in the range 1000–1200°C.

¹Carborundum Universal Ltd, Industrial Ceramics Division, 47 Sipcot Industrial Complex, Hosur – 635126, Tamilnadu, India

²Materials Research Centre, Department of Engineering and Applied Science, University of Bath, Bath BA2 7AY, UK

*Corresponding author, email jiten_kar@hotmail.com



1 X-ray diffraction pattern of pigment powder ZSPR, heat treated at 900°C for 2 h

Powders which after the various heat treatments generated an intense or attractive colour were considered for further characterisation using X-ray diffraction (XRD) and scanning and transmission electron microscopy (SEM, TEM). Fired samples were fabricated either in powder form or as partially sintered ceramic material. The calcined/sintered pigment powders were then ground for different periods using zirconia grinding media and water as the liquid suspension. The purpose of milling was to reduce the particle size to a predetermined level (average particle size 5–10 µm), as required for a particular ceramic application, for example glass, tile or sanitaryware.

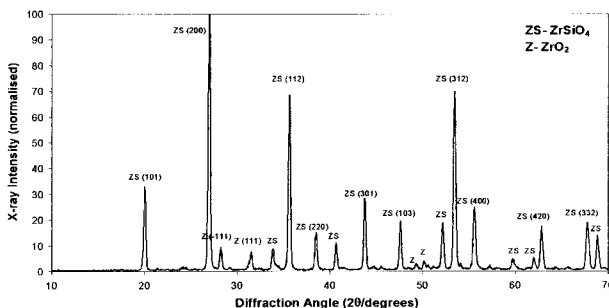
Characterisation

X-ray diffraction

XRD analyses of the samples were performed on a Philips PW1730/00 diffractometer using monochromatic Cu $K\alpha$ radiation ($\lambda=0.154060$ nm) and with generator voltage and current of 40 kV and 25 mA respectively. X-ray scans were made between 2θ angles of 10 and 80° . A scan speed of 1.0 s per step and a step size of 0.02° were used. An external standard method^{9,10} was used to calculate the weight fraction of unreacted ZrO₂ in the mixture.

Electron microscopy

The structure of the Pr–zircon samples was examined using a Jeol JSM 6310 analytical scanning electron microscope fitted with a 10/85 link microanalysis system, manufactured by Oxford Instruments. Further examination of the powder microstructure was carried out using a Jeol 2010 TEM to investigate the presence of defects, the nature of the grain boundaries and any internal defect structures. Generation of colour is generally associated with the presence of lattice defects, usually in the form of complex vacancies and substitutional ion species.¹¹



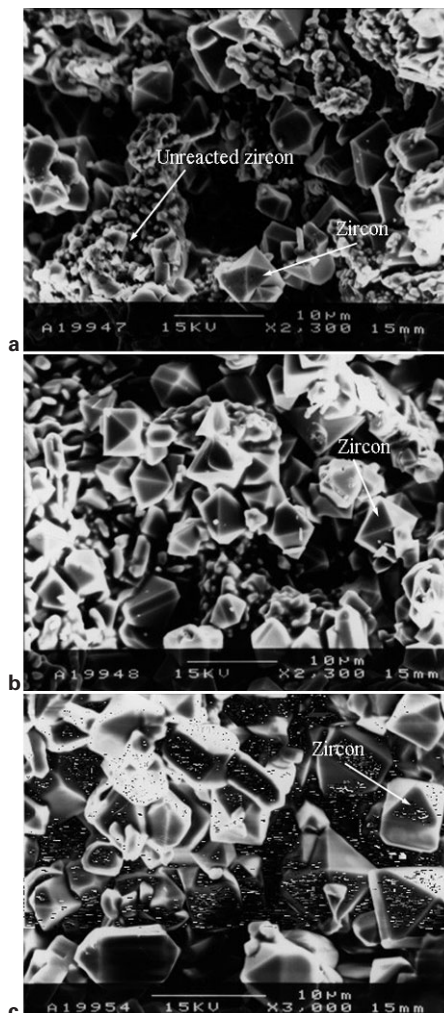
2 X-ray diffraction pattern of pigment powder ZSPR2, heat treated at 1000°C for 2 h

Results and discussion

X-ray diffraction

In order to determine the different phases present in the calcined samples, X-ray diffraction analysis was carried out, and examples of the resulting patterns are given in Figs. 1 and 2, which show the diffraction data from samples calcined at 900 and 1000°C respectively.

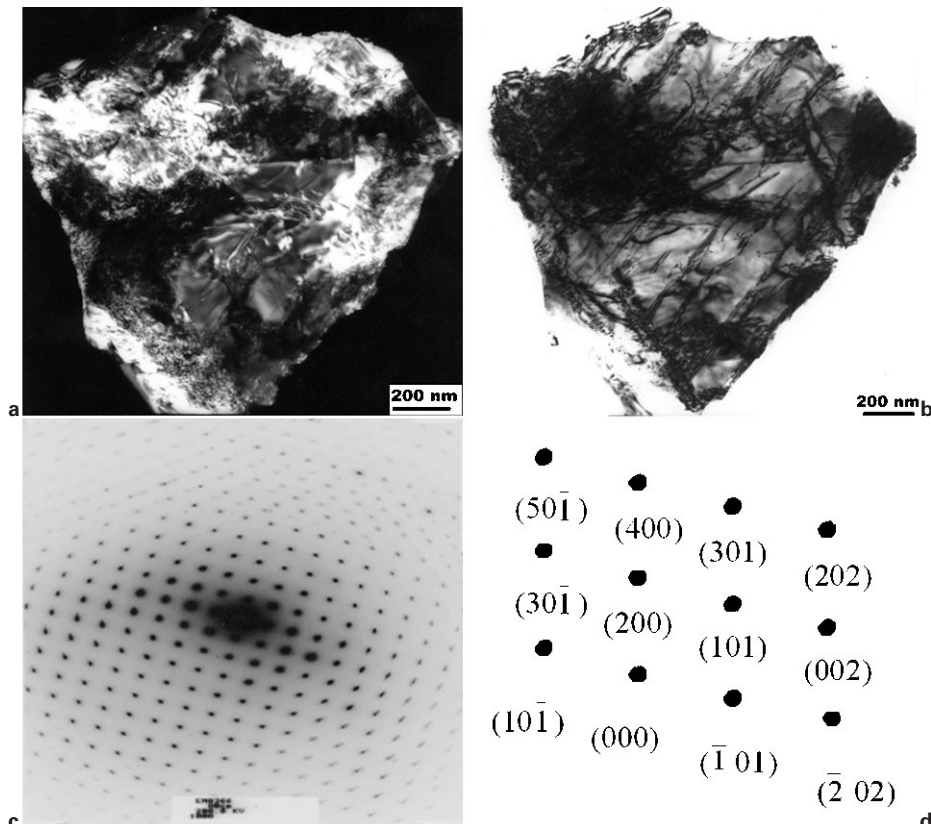
The XRD pattern of the sample shown in Fig. 1 indicates that the powder was found to consist of zircon and a large amount of unreacted zirconia and silica. The same pattern was obtained for the sample calcined at 950°C. The XRD trace of the sample obtained at 1000°C



3 SEM image of Pr-zircon crystals after calcination at 1000–1200°C with 2 h soaking

Table 1 Samples used for calcination: NaF fluxing agent at 5 wt-% of total mixture

Sample	Calcination temp., °C
ZSPR	900
ZSPR1	950
ZSPR2	1000
ZSPR3	1100
ZSPR4	1200
ZSPR5	1050



4 Dark (A) and bright (B) field images of Pr-zircon sample diffraction pattern with indexing (C) after calcination at 1000°C: tilt angle +25.5°, magnification $\times 40\,000$

(Fig. 2) shows that the powder was found to consist of zircon, although traces of zirconia were also present. Similar diffraction patterns were obtained from samples treated at 1100 and 1200°C. Absence of peaks for praseodymium oxide indicates that it has diffused into the host crystal to form a solid solution.

Calculation of weight fraction of unreacted zirconia

The weight fraction of unreacted zirconia w_α was calculated and is presented below for $Zr_{0.95}Pr_{0.05}SiO_4$ calcined at 1000°C. From Fig. 2, the high intensity peak of zirconia can be seen to be $Z(-111)$. With I_α as the intensity of the ZrO_2 peak in the heterogeneous mixture (266 from the raw scan) and $I_{\alpha p}$ the intensity of the pure ZrO_2 peak (3147 from the raw scan), the weight fraction of unreacted zirconia w_α was calculated as follows^{9,10}

$$\frac{I_\alpha}{I_{\alpha p}} = \frac{w_\alpha(\mu_\alpha/\rho_\alpha)}{w_\alpha(\mu_\alpha/\rho_\alpha) - (\mu_\beta/\rho_\beta) + \mu_\beta/\rho_\beta} \quad (1)$$

where μ_α and μ_β are the linear absorption coefficients and ρ_α and ρ_β the densities respectively of ZrO_2 and $ZrSiO_4$, μ_α/ρ_α the mass absorption coefficient of ZrO_2 , and μ_β/ρ_β the mass absorption coefficient of $ZrSiO_4$.

The mass absorption coefficients for ZrO_2 and $ZrSiO_4$ were found to be 275 and 176 respectively and were calculated using the equation^{9,10}

$$\mu = \frac{n}{V_c} \sum (\mu_a)_I \quad (2)$$

where n is the number of molecules in the unit cell of the

compound, V_c the volume of the unit cell, and

$$\sum (\mu_a)_I \rightarrow \left(\frac{\mu}{\rho} \right)_I \left(\frac{A}{N} \right)$$

where $(\mu/\rho)_I$ is the mass absorption coefficient of the individual element using $Cu K_\alpha$ radiation, A the atomic number of the element and N Avogadro's number (6.023×10^{23}).

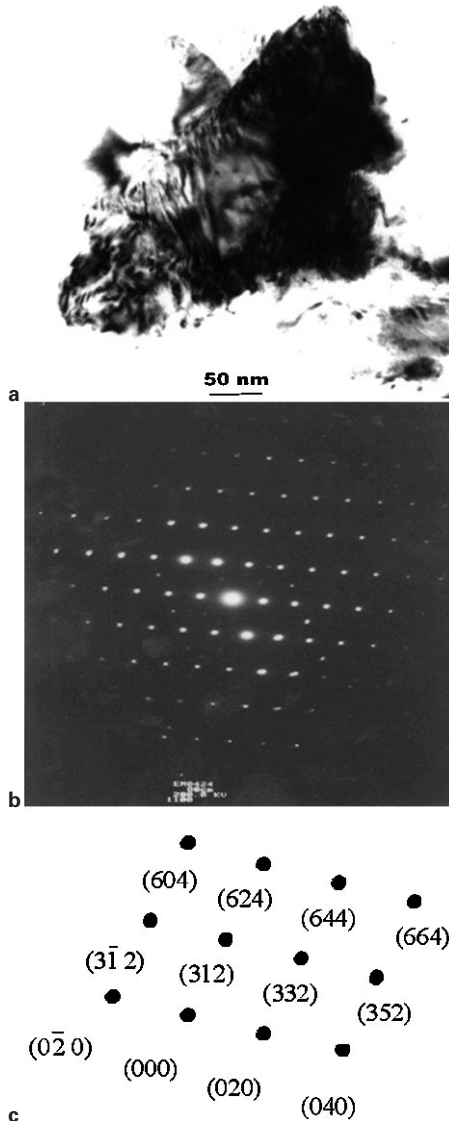
Using equation (1) and substituting the values of I_α , $I_{\alpha p}$, μ_α/ρ_α and μ_β/ρ_β , w_α was calculated to be 0.0559, as follows:

$$\frac{266}{3147} = \frac{w_\alpha \times 275}{(w_\alpha \times 98.41) + 176.6}$$

The weight fraction of unreacted zirconia present in the sample after calcination at 1000°C was thus found to be 0.056. Similarly, the weight fractions of unreacted zirconia at 1100 and 1200°C were found to be nearly 0.056, as the X-ray diffraction intensities obtained were almost the same, as described above. It is important to note that the external standard method is not applicable to samples containing more than two phases. At 900 and 950°C, the samples consist of multiple phases (more than two phases) with little formation of zircon. Thus the method presented was not applicable to calculation of the weight fraction of unreacted zirconia at these temperatures.

Scanning electron microscopy

SEM images showing the morphology of samples generated at different temperatures are shown in Fig. 3. The images from samples treated at different



5 TEM image of Pr-zircon crystal diffraction pattern with indexing after calcination at 1100°C: tilt angle +12·1°, magnification $\times 30\,000$

calcination temperatures indicate that the growth of the tetrahedral shaped crystals is enhanced by the addition of mineraliser. At 1000°C two size ranges of crystal were evident, whereas at a temperature of 1100°C the crystals were of uniform size. At a temperature of 1200°C distinct growth of crystals was evident. Unreacted zirconia was also observed in the micrographs, in good agreement with the results obtained by XRD, where the intensity peaks due to ZrO_2 were calculated as being equivalent to an unreacted 0·056 weight fraction.

Transmission electron microscopy

Investigation of the nature of grain boundaries and lattice defects was performed using TEM at 200 kV. TEM micrographs of samples after calcination at different heat treatment temperatures are shown in Figs. 4–6. The dark contrast lines and loops in the crystal are caused by dislocations generated by the milling process and subsequently modified by calcination treatment.

From the TEM micrographs of crystals treated at different temperatures it was seen that at 1000 and

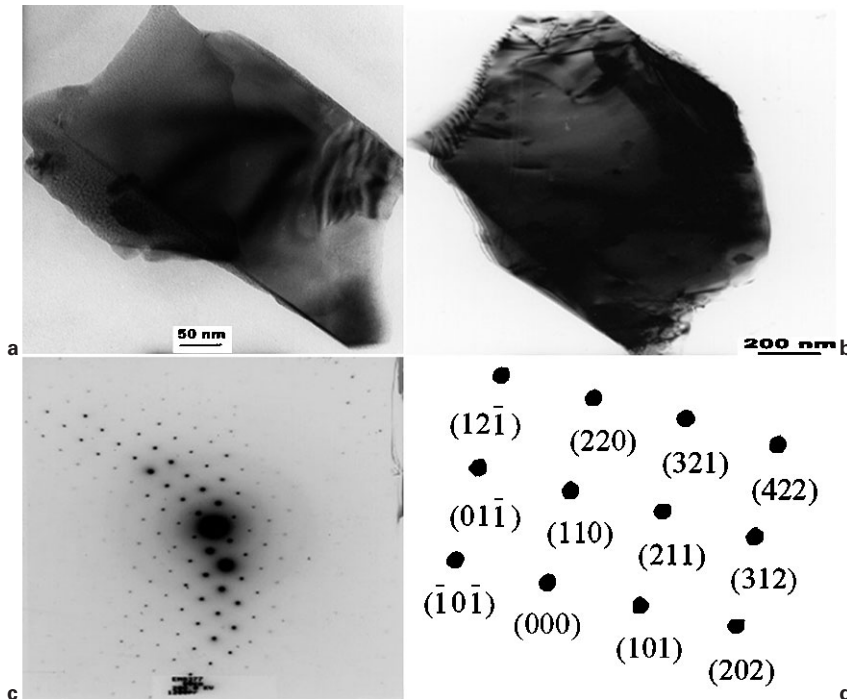
1100°C there were numerous dislocations and extensive elastic strain, whereas at 1200°C the crystal is almost free of dislocations and elastic strain. Indexing of the electron diffraction pattern from the samples treated at each temperature shows the same type of crystal structure (tetragonal) but with different orientation. Lattice defects are generated as a result of distortion in the lattice and determine the intensity of the colour obtainable in a particular system. The intense colour would be expected in a system when more lattice defects are present.

Colour mechanism

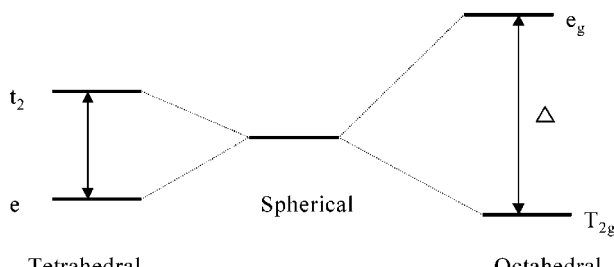
The mechanism for colour formation in the zircon host lattice can be explained on the basis of crystal field splitting.^{11–13} The colour produced by an ion is due to the d or f electrons moving across the energy gap created by the splitting of the crystal field. Rare earth oxides (Pr_6O_{11}) have seven f orbitals which have the same energy level in the ground state. When Pr_6O_{11} is put in a host lattice such as zircon, Pr^{3+} replaces one of the Zr cations of the host lattice. The cation it will be able to substitute/replace depends on the size (ionic radius) of each of the ions and the net energy of the final system after substitution has occurred. Sodium fluoride NaF has been used in the present work as a mineraliser to aid the formation of the host lattice structure at a lower calcination temperature, and also to achieve the electroneutrality required in the ion substitution process.

Consequently, owing to this interaction of f electrons of the rare earth ion with the surrounding electrons, the f orbitals split into two groups, one having higher energy than the other (Fig. 7). There are two possible types of orbital energy splitting. One is tetrahedral splitting where the rare earth ion is surrounded by a tetrahedron of O^{2-} ions and the second is octahedral splitting where the rare earth ion is surrounded by an octahedron of O^{2-} ions. The structure of the praseodymium doped zircon crystal is given in Fig. 8. The magnitude of splitting for ions in an octahedral configuration is greater than in tetrahedral because six negative ions are involved compared to four in the tetrahedron, and they are closer to the cation resulting in strong crystal field splitting. The transition of energy from the higher energy level to the lower energy level gives rise to the characteristic colour if this characteristic energy falls into the visible spectrum. In the present case, since the energy falls in the yellow region of the spectrum, a yellow colour is generated and because many such events take place the colour is intense. The degree of crystal field splitting will depend on the geometry of the surrounding ions and how close they are to the active cation. This indicates that any specific rare earth cation can exhibit different colours in different host crystals, owing to the difference in transition energies.

In Fig. 7, T_{2g} is the set of d orbitals having lower energy and e_g is the set of d orbitals having higher energy in the octahedral crystal field splitting; t_2 is the set of d orbitals having higher energy and e is the set of d orbitals having lower energy in the tetrahedral crystal field splitting. In an octahedral field the T_{2g} set have a lower energy and the e_g set a higher energy with respect to the spherical group, whereas in a tetrahedral field the condition is reversed. Crystal field splitting, that is the separation of lower and upper energy levels, is known as



6 TEM image of Pr-zircon crystal diffraction pattern with indexing after calcination at 1200°C: tilt angle +12·1°, $\times 30\,000$



7 Example of crystal field splitting of chromophore ion in presence of host crystal

Δ in octahedral splitting. In the case of tetrahedral splitting it is characterised as $4/9\Delta$.

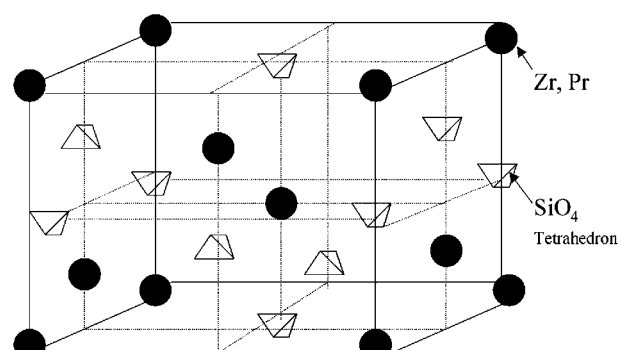
Conclusions

1. Incorporation of Pr_6O_{11} into the zircon host lattice by substitutional solid solution produced intense yellow coloration at calcination temperatures in the range 1000–1200°C.

2. From the XRD patterns of samples treated at 900 and 950°C, large amounts of unreacted zirconia were found to be present. At 1000, 1100 and 1200°C, zircon was found to be the major phase although traces of zirconia were still detected.

3. SEM micrographs revealed the presence of tetrahedral crystals and unreacted zirconia whereas TEM micrographs show the presence of dislocations and elastic strains in the samples at different calcination temperatures.

4. Praseodymium doped zircon pigment is an excellent example of crystal field colour. The colour produced in this case is due to the f electrons moving across the energy gap created by the crystal field splitting of the f orbitals of the colouring ion Pr^{3+} . The magnitude of the splitting depends on the interactions of f electrons of the



8 Structure of praseodymium doped zircon crystals

Pr^{3+} ion with the surrounding electrons and also determines the intensity of the colour. In a strong crystal field splitting, the intensity of the colour will be more intense, when compared to a weak crystal field splitting, owing to the involvement of a greater number of f electrons in the transition process.

Acknowledgements

The authors are grateful to the European Commission for providing financial assistance and to Treibacher Auermet, Austria for supply of the raw materials.

References

1. D. R. Eppler and R. A. Eppler: *Ceram. Eng. Sci. Proc.*, 1997, **18**, 139–149.
2. K. H. Hudson Winbow and J. Cowley: *Ceram. Eng. Sci. Proc.*, 1996, **17**, 102–110.
3. K. Shaw: 'Ceramic colours and pottery decoration'; 1962, London, MacLaren and Sons.
4. C. Decker: *Ceram. Eng. Sci. Proc.*, 1990, **11**, 307–313.
5. R. W. Batchelor: *Trans. J. Br. Ceram. Soc.*, 1974, **73**, 297–301.

6. R. A. Eppler: in 'Physics of electronic materials. Part B', (ed. L. L. Hench and D. B. Dove), 1021–1045; 1972, New York, NY, Marcel Dekker.
7. J. Bretka, R. G. Bowman and T. Brown: *J. Aust. Ceram Soc.*, 1981, **17**, 37.
8. F. Bondioli, A. B. Corradi, A. M. Ferrari and T. Manfredini: *J. Am. Ceram. Soc.*, 2000, **83**, 1518–1520.
9. 'International tables for X-ray crystallography', 162; 1962, Birmingham, Kynoch Press.
10. B. D. Cullity: 'Elements of X-ray diffraction', 2nd edn; 1978, London, Addison-Wesley.
11. R. Tilley: 'Colour and optical properties of materials'; 1999, Chichester, Wiley.
12. K. Nassau: 'The physics and chemistry of color (the fifteen causes of color)'; 1983, New York, NY, Wiley.
13. F. Stern: 'Elementary theory of the optical properties of solids'; 1963, New York, NY, Academic Press.